Accepted for publication in *the Astrophysical Journal Letters*
July 8, 2003

The Bursting Behavior of 4U 1728-34: Parameters of a Neutron Star and Geometry of a NS-disk system

Nickolai Shaposhnikov[1], Lev Titarchuk[1,2] and Frank Haberl[3]

ABSTRACT

We analyze a set of Type I X-ray bursts from the low mass X-ray binary 4U 1728-34, observed with *Rossi X-ray Timing Explorer* (RXTE). We infer the dependence of the neutron star (NS) mass and radius with respect to the assumed distance to the system using an analytical model of X-ray burst spectral formation. The model behavior clearly indicates that the burster atmosphere is helium-dominated. Our results strongly favor the soft equation of state (EOS) of NS for 4U 1728-34. We find that distance to the source should be within 4.5-5.0 kpc range. We obtain rather narrow constrains for the NS radius in 8.7-9.7 km range and interval 1.2-1.6 $M_{\odot}$ for NS mass for this particular distance range. We uncover a temporal behavior of red-shift corrected burst flux for the radial expansion episodes and we put forth a dynamical evolution scenario for the NS–accretion disk geometry during which an expanded envelope affects the accretion disk and increases the area of the neutron star exposed to the Earth observer. In the framework of this scenario we provide a new method for the estimation of the inclination angle which leads to the value of $\sim 50°$ for 4U 1728-34 .

Subject headings: accretion, accretion disks—stars:fundamental parameters—stars:individual(4U 1728-34) — X-ray: bursts

[1]George Mason University, Center for Earth Observing and Space Research, Fairfax, VA 22030; nshaposh@scs.gmu.edu; lev@xip.nrl.navy.mil

[2]NASA/ Goddard Space Flight Center, Greenbelt MD 20771, USA; lev@lheapop.gsfc.nasa.gov

[3]Max-Planck-Institut für extraterrestrische Physik, Giessenbachstraße, 85748 Garching, Germany, fwh@mpe.mpg.de

1. Introduction

A low mass X-ray binary (LMXB) system consists of a neutron star (NS) which accretes matter through Roche lobe overflow from an evolved low-mass secondary star. 4U 1728-34 has been recognized as a classical LMXB because it exhibits a wide range of observational characteristics which are attributed to LMXBs [see e. g. Lewin, van Paradijs & Taam (1993)]. In particular, it exhibits regular thermonuclear explosions of accreted matter on the NS surface [Type I X-ray bursts, see Strohmayer & Bildsten (2003) for the latest review]. High-frequency quasi-periodic oscillations (kHz QPO) in persistent emission [Ford & van der Klis (1998); Mendez & van der Klis (1999)], and 363 Hz burst oscillation [Strohmayer et al. (1998), Franco (2001), van Straaten et al. (2001), hereafter VS01] were revealed in burst emission from 4U 1728-34 using Fourier analysis of the high time-resolution RXTE data. So far, no optical counterpart for this X-ray source has been found. Although 4U 1728-34 is believed to be located several kiloparsecs from the Earth, no accurate estimation of the distance to the source is currently available. The theory of X-ray spectral formation during the expansion and contraction stages of the bursts was developed in Titarchuk (1994) and Shaposhnikov & Titarchuk (2002), hereafter T94 and ST02 respectively. This theory was first applied to EXOSAT data in Haberl & Titarchuk (1995), hereafter HT95, for the LMXBs 4U 1705-44 and 4U 1820-30. In Titarchuk & Shaposhnikov (2002), hereafter TS02, three bursts from Cyg X-2 were analyzed. In this work we employ the methodology, developed in TS02 to analyze a set of 26 bursts from 4U 1728-34, previously analyzed in VS01 to search for burst oscillations. Compared with Cyg X-2 (TS02), the 4U 1728-34 burst data have the advantage of high quality counting statistics as well as a larger number of burst events.

A brief description of the data used in the analysis is given in §2. We present the model and the results of its application to the burst data of 4U 1728-34 in §3. Specifically, we obtain the dependence of the NS mass on the radius as error contours, calculated for the set of distances to the system taken from reasonable interval. In §4 we offer an evolution scenario for the NS - accretion disk geometry, which can explain the existing controversy between the Eddington limit for the peak flux and the flux behavior during the bursts with radial expansion (Strohmayer & Bildsten 2003). In §4 we also present estimates for the inclination angle of the system. We discuss our results and come to conclusions in §5.

2. Observations

We analyzed the data collected by the Proportional Counter Array, (PCA; Jahoda et al. 1996), the main instrument on board the *RXTE*. Generous amount ($>$ 1100 ksec) of *RXTE* observational time was devoted to 4U 1728-34. More than 70 bursts were detected.

For our analysis we selected the subset of bursts based on statistical equivalence and PCA data configuration homogeneity, namely, when all five detectors of PCA are operational and detailed spectral analysis on a subsecond time scale is possible. The selected events occurred during three periods: 15 March - 1 February 1996 (Proposal ID 10073), 19 September - 1 October 1997 (Proposal ID 20083), and 28 February - 10 June 1999 (Proposal ID 40027). A total of 26 Type I bursts were selected. Due to its exotic nature we excluded the second burst detected on 26 September 1997 (Observation ID 20083-01-04-00, burst 19 according VS01 numbering).

3. Data analysis and results

We extract spectral slices from the Burst Catcher Mode for consecutive 0.125 sec time intervals for each burst. We obtain the spectrum of the persistent emission using a 300-500 second time interval prior to a particular burst and we input resulting spectra as a background to distinguish the burst radiation component. We use fixed hydrogen column of $N_H = 1.6 \times 10^{22}$ provided by HEASARC[4] to model Galactic absorption. The dead-time corrections is applied to all spectra. We fit the burst emission component using a blackbody model. This is justified because the X-ray burst spectrum deviates from the blackbody-like shape only in the soft part $\lesssim 1$ keV (T94 and ST02). The quality of the fits is quite good for all spectra except the particular contraction episodes when the luminosity is very close to the Eddington and the photospheric radius changes rapidly along with the outgoing spectrum shape. We calculate model flux between 0.01 and 100 keV. Errors for parameter estimations from spectral fits are calculated for 68% (1σ) confidence level. For the interpretation of the spectral fit results we utilized the theoretical model for the color temperature of the spectra from the burst cooling phase. The underlying formalism is developed in T94 and TS02. Here we present the final formula for the color temperature kT_∞(see Eqs. 7-8 in TS02)

$$kT_\infty = 2.1\, T_h \{lm[(2 - Y_{He})(z+1)^3 r_6^2]^{-1}\}^{1/4} \mathrm{keV} \tag{1}$$

where m is the NS mass in units of solar mass, r_6 is the NS radius in units of 10 km, Y_{He} is the helium abundance, $l = L/L_{Edd}$ is the dimensionless luminosity in units of the Eddington luminosity. T_h is the color (hardening) factor, which depends on l, and Y_{He} (TS02). Parameters of the model are m, r_6, Y_{He} and d_{10} - distance to the object in units of 10 kpc. The dimensionless luminosity (Eddington ratio) is expressed by

$$l = 0.476\, \xi_b\, d_{10}^2 F_8 (2 - Y_{He})(z+1)/m, \tag{2}$$

[4]http://heasarc.gsfc.nasa.gov/cgi-bin/Tools/w3nh/w3nh.pl

where ξ_b is an anisotropy factor, $F_8 = F/(10^{-8}$ erg cm^{-2} s$^{-1})$ is the observed bolometric flux. Equations (1) and (2) describe the functional dependence of the observed kT_∞ on the observed flux F_8 for the set of input parameters m, r_6, Y_{He} and d_{10}. In the next section we put forth the NS-accretion disk geometry scenario and infer the behavior of ξ_b during a burst with radial expansion. In this proposed scenario, the transition from the expansion stage to the decay stage is described graphically on the upper panel of Figure 1. At the beginning of the decay stage, immediately after the expansion stage ends, the entire star is exposed to the observer. We do not need any correction due to the system geometry, which means that $\xi_b = 1$ in this case. Then at some moment $t = t^*$ accretion disk recedes (reaches the star surface) and a certain part of the NS is obscured by the disk for the observer. The anisotropy factor ξ_b^* that quantitatively takes into account this occultation effect is more than one in this case. In terms of functional dependence of kT_∞ upon F_8 the flux domain consists of three intervals. For $F_8 > \xi_b^* F_8^*$ the entire star is open and $\xi_b = 1$. The flux level $\xi_b^* F_8^*$ from the NS surface is related to the star-disk position when the lower NS hemisphere starts to get covered by the disk. Through the decay stage the temperature should be calculated using formulae (1) and (2) where $\xi_b = \xi_b^* > 1$. Thus the model formulated in this way acquires two more parameters, the anisotropy factor during occultation ξ_b^* and dimensionless flux F_8^* at the moment when occultation occurs. Our analysis shows that constant values of these parameters for all bursts with radial expansion are consistent with observations. We use $\xi_b^* = 1.2$ that is estimated using the expansion stage evolution (see § 4). The best-fit value for $F_8^* = 5.7$ does not significantly depend on the distance either.

We combine fluxes and temperatures for all 26 bursts and fit the model to the the entire data set in the range $1.0 < F_8 < 9.5$, which approximately corresponds to $0.1 < l < 0.9$. We use the lower limit to exclude the data points with large errors. We put the upper limit on l because of the restricted validity of the model for $l \sim 1$ where expansion of the atmosphere can occur. We use a set of values for the distance between 4 and 5 kpc. We found that our analytical model gives statistically acceptable fit only when $Y_{He} > 0.9$. In fact, for lower Y_{He} the slope of the model color temperature dependence on F_8 is steeper than that is dictated by the data (see Fig. 2). The model with hydrogen-reach gas composition fails to describe the data, particularly, due to the strong dependence of the hardening factor on the Eddington ratio l. A given change in flux represents a larger change in the Eddington ratio in an H-atmosphere than that in an He-atmosphere because the value of L_{Edd} is smaller for an H-atmosphere. We consider this fact as a strong argument for NS atmosphere in 4U 1728-34 to be helium dominated and further we assume $Y_{He} = 1.0$ during the whole proceeding analysis. In Figure 2 we present the data and the best-fit model for the case of $d_{10} = 0.45$ for which we obtain $M_{NS} = 1.25^{+0.06}_{-0.04}\,M_\odot$ and $R_{NS} = 9.00^{+0.17}_{-0.28}$ km. The best-fit values of NS mass and radius and error contours for 68%, 90% and 99% confidence levels are obtained for

each fit and they are presented in Table 1 and Figure 3. The number of degrees of freedom is 1418 and thus the acceptable fits must satisfy the condition that $\chi^2_{red} = \chi^2/1418 \leq 1.0$. This condition is not satisfied for distances higher than 5 kpc for which χ^2_{red} grows very rapidly. This fact suggests that probability for NS mass to be higher than 1.6 $M_\odot$ is very low. The dashed line in Figure 3 presents the dependence of the inner disk radius R_{in} on the NS mass m, derived for 4U 1728-34 using the transition layer model (TLM) for QPOs detected in the persistent state from LMXBs (Titarchuk & Osherovich 1999; Li et al. 1999): $R_{in} = 9 \times m^{1/3}$ km. Our values of the NS radius are in good agreement with the TLM. Based both on this fact and on statistical behavior of the model we can conclude *that 4.5 - 5.0 kpc is the most probable interval for the distance to the source, that relates to 8.7-9.7 km and 1.2-1.6 $M_\odot$ ranges for R_{NS} and M_{NS} respectively.*

4. Dynamic evolution of the system geometry during the expansion stage

We investigate the temporal evolution of the burst atmosphere photospheric radius for each individual burst in the manner similar to TS02 and HT95. Choosing particular values of distance and NS mass (obtained from the model fit) we find the radius [i.e. solve equation (7) of TS02] for each spectral slice. The evolution of the NS photospheric radius during the burst event is shown in Figure 1 for the case of $d_{10} = 0.45$. We present radius (diamonds) and observed flux (empty circles) values versus time for burst 9, according to the VS01 numbering convention (observation ID 10073-01-06-00). The data were rebinned with 0.25 second time resolution for presentation purpose. Filled circles represent the red-shift-corrected flux for each data point. This red-shift recalculated flux, is the flux which would be detected by an observer situated on the NS photosphere. Restoration of the red-shift corrected flux reveals distinctive features which are barely seen in the observed flux behavior. After the initial rise of the burst, the flux levels off and stays constant for more than a second while the radius increases gradually. After the radius reaches its maximum, a second rise in the flux occurs. The flux reaches its maximum value when radius begins to fall quickly in contrast to the initial flux plateau. After that, flux decays exponentially, indicating the end of the expansion stage, and radius levels off.

The above analysis clearly indicates that the flux emitted in the direction of the Earth, (when measured locally at the NS surface), is not constant throughout the expansion stage. This behavior of the burst peak flux was found to be common for many bursters [see VS01, Galloway et al. (2002)]. If the system geometry remains unchanged, the mentioned flux behavior is in contradiction with the Eddington limit for the radiation power from a stellar atmosphere. We argue that the expanded burst envelope interacts strongly with the inner

accretion disk. The evolution of the system geometry through the burst event is displayed in the upper part of Figure 1. Before the burst the accretion disk extends down to the surface of NS (stage a), *covering the lower part of the NS, which is not exposed to the Earth observer*. Then the burst starts and the atmosphere expands (stage b). At this moment, the inner part of the disk is swept away by the burst radiation pressure in excess of Eddington flux. This stage corresponds to the initial plateau of the red-shift corrected flux versus time. After the photosphere begins to contract, the second rise in the red-shift corrected flux starts, effectively indicating that *the lower NS hemisphere appears from behind the accretion disk*. Indeed, the free fall velocity is much higher than the radial propagation velocity component in the disk. After the touchdown of the burst envelope, the NS-disk configuration corresponds to the case (c). We assume that the red-shift corrected flux obtained for geometry (b) is the critical (upper limit) hemisphere flux. Obviously, the red-shift corrections depend on the NS mass and radius. Using the standard disk theory (Shakura & Sunyaev 1973) one can estimate the expansion stage duration required for sufficient disk material evacuation as

$$\mathcal{T}_{Exp} \approx 10^{-6} m/(\alpha \dot{m}^2 \varepsilon) \ \ s, \tag{3}$$

where α is efficiency of the radial momentum transfer, $\dot{m}$ is the mass accretion rate in units of critical mass flux value and $\varepsilon \approx 0.03 \sim 0.05$ is a burst flux fraction transformed into the potential energy of ambient gas (see e.g. ST02). For burst sources the persistent mass accretion rate in the disk is believed to be $\dot{m} = 0.1 \sim 1$ [see e. g. Lewin, van Paradijs & Taam (1993)]. Values for $\alpha \sim 0.1$ are widely used in the astrophysical community for LMXB. Under these assumptions it takes only a small fraction of a second ($\mathcal{T}_{Exp} \ll 0.1$ s) to push the inner disk edge out, while observed expansion episodes of strong bursts from 4U 1728-34 usually last more than a second. This simple estimate suggests that the expanded NS atmosphere effectively push accretion disk outward.

As long as the total NS luminosity during expansion stage (the Eddington luminosity) is constant the observed radiation flux is higher in geometry (c) than in (a) and (b). Assuming that the NS radiates at the Eddington limit, the ratio of fluxes detected from the direction at inclination angle i from the normal to the accretion disk in geometries (b) and (c) is

$$\tilde{F}_b/\tilde{F}_c = H(i)/H(0), \quad H(i) = \int_{i-\pi/2}^{\pi/2} \cos\omega d\omega \int_{-\pi/2}^{\pi/2} I(\mu) \cos^2\psi d\psi, \tag{4}$$

where ω and ψ are starcentric coordinates, $\mu = \cos\omega\cos\psi$ and $I(\mu)$ describes the angular intensity distribution law (see Sobolev 1975 for details). The tilde denotes the fact that value of flux was corrected for redshift. For the burst, presented in Figure 1, we have $\tilde{F}_b \simeq 1.3\times10^{-7}$ erg/cm^2 and $\tilde{F}_c \simeq 1.55\times10^{-7}$ erg/cm^2. Assuming $I(\mu) = \text{const}$ (the Lambert law), we obtain $\tilde{F}_b/\tilde{F}_c = (1+\cos i)/2$ which leads to an estimate of the inclination angle $i \sim 50°$. This result

is also close to that for the Chandrasekhar angular distribution, $I = I_0(1 + 2.06\mu)$. We can apply the value of $\tilde{F}_c$ for the quantitative assessment of the distance to the source. The peak of the red-shift corrected flux $\tilde{F}_c$ corresponds to the state when the burst atmosphere subsides on the NS surface. The anisotropy factor is estimated as $\xi_b = \tilde{F}_c/\tilde{F}_b \simeq 1.2$. We use this value as the anisotropy factor ξ_b^* in the a-geometry .

5. Discussion and Conclusions

In this *Letter* we offer a sophisticated analysis of the burst expansion events. Accounting for the general relativistic (GR) effects reveals the dynamics and geometry of the NS-disk system and consistently explains the controversy between theory and the behavior observed during the expansion episodes of X-ray bursts. As a direct outcome of the proposed geometric scenario we obtain the distance and estimate the inclination angle of the system. The derived mass-radius relation depends on the assumed anisotropy. For example, without taking into account of anisotropy, $\xi_b = 1$ (conventual approach) we obtain $M/M_\odot = 1.29$ and $r = 7.8$ km for $d = 4.5$ kpc while accurate anisotropy corrections implemented in §3 result in $M/M_\odot = 1.25$ and $r = 9.0$ km.

The statistical behavior of our model clearly rules out values of helium abundance lower than 0.9. We could not find the set of model parameters including the distance that would give an acceptable value of χ^2 for $Y_{He} < 0.9$. The lower values of helium abundance gives much steeper temperature versus flux functional dependence than it is dictated by the data. Furthermore, in earlier observations of 4U 1728-34 Basinska et al. (1984) found that helium was probably the main source of nuclear fuel for the bursts and that any contribution from hydrogen was small. Our data analysis confirms the results of Basinska et al. and gives another argument for a helium-reach atmosphere in 4U 1728-34. Our results also favor the soft EOSs [Baym & Pethick (1979)].

We conclude that (1) the application of our analytical model to the data leads to the determination of the NS mass and radius as a function of the distance to the system. For the range of allowed distances 4.5-5.0 kpc we obtain rather narrow constrains for the NS radius in 8.7-9.7 km range and wide interval 1.2-1.6 $M_\odot$ for NS mass (see also discussion in TS02 and Strohmayer & Bildsten 2003); (2) the consistent evolution scenario for the NS - accretion disk geometry, which explains the variation of the peak flux during the radial expansion stage; (3) our geometrical model enables us to estimate; the inclination angle of the system to $i \sim 50^\circ$ with respect to the Earth observer.

We acknowledge the fruitful and constructive discussion with the referee.

REFERENCES

Baym, G., & Pethick, C. 1979, Ann. Rev. Astr. Ap. 17, 415

Basinska, E.M., et al. 1984, ApJ, 281, 337

Di Salvo, T., Iaria, R., Burderi, L.,& Robba N. R. 2000, ApJ, 542, 1034

Ford, E. C., & van der Klis, M. 1998, ApJ, 506, L39

Franco, L. M. 2001, ApJ, 554, 340

Galloway, D. K., et al. 2003, ApJ, 590, 999

Haberl, F., & Titarchuk, L. 1995, A&A, 299, 414 (HT95) 1999, Astron. Lett, 25, 269

Jahoda, K., et al. 1996, Proc. SPIE, 2808,59

Lewin, W.H. G., van Paradijs, J., & Taam, R.E. 1993, Space Sci. Rev., 62, 223

Li, X., et al. 1999, Phys. Rev. Lett., 83, 3776

Mendez, M., & van der Klis, M. 1999, ApJ, 517, L51

Shakura, N.I., Sunyaev, R. A. 1973, A&A, 24, 337-355

Shaposhnikov, N., & Titarchuk, L. 2002, ApJ, 567, 1077 (ST02)

Sobolev, V.V. 1975, Light Scattering in Atmospheres (Oxford: Pergamon)

Strohmayer, T.E., Zhang, W., Swank, J.H. & Lapidus, I.I. 1998, ApJ, 503, L147

Strohmayer, T.E., Bildsten, L. 2003, in "X-ray Binaries", in press, astro-ph/0301544

Titarchuk, L. 1994, ApJ, 429, 330

Titarchuk, L., & Osherovich, V. 1999, ApJ, 518, L95

Titarchuk, L., & Shaposhnikov, N. 2002, ApJ, 570, L25 (TS02)

van Straaten, S., van der Klis, M., Kuulkers, E., & Mendez, M. 2001, ApJ, 551, 2 (VS01)

Table 1. NS Masses and Radii from Model Fits for 4U 1728-34.[b]

Distance kpc	m $M_\odot$	R_{NS} km	χ^2_{red} χ^2/DoF
4.00	0.91 ± 0.02	$8.66^{+0.08}_{-0.10}$	0.963
4.25	$1.06^{+0.03}_{-0.02}$	$8.92^{+0.10}_{-0.13}$	0.963
4.50	$1.25^{+0.06}_{-0.04}$	$9.00^{+0.17}_{-0.28}$	0.963
4.75	1.48 ± 0.04	8.86 ± 0.23	0.972
5.00	1.61 ± 0.02	$9.60^{+0.12}_{-0.11}$	1.102

[a]errors are given for 90% of confidence

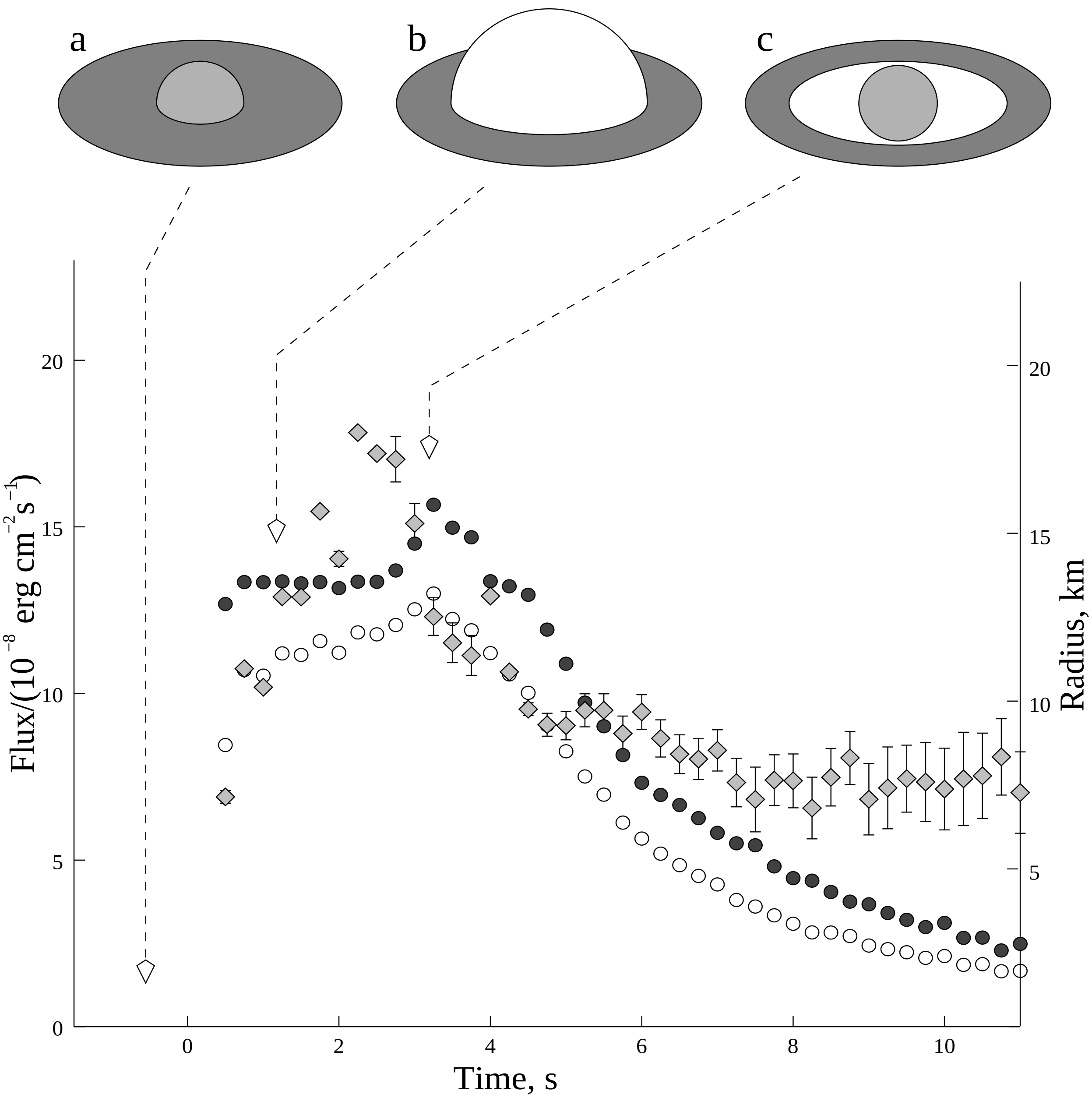

Fig. 1.— Geometry evolution of the burst through radial expansion. White circles present observed bolometric flux. Filled circles present GR corrected flux. Photospheric radii inferred for the pure helium atmosphere and distance of 4.5 kpc are shown by diamonds. Upper panel displays a cartoon diagram of different states of a NS-accretion disk system. Dashed arrows point to different stages of the burst.

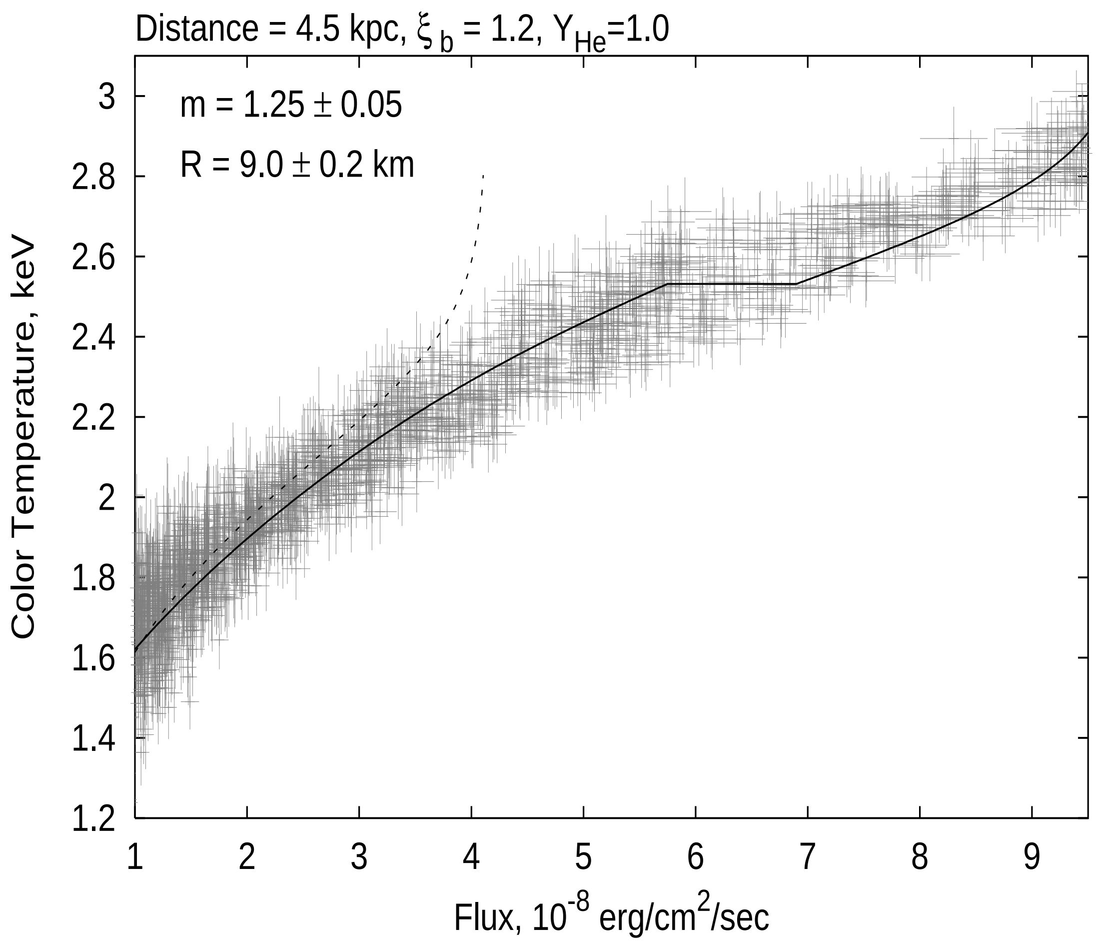

Fig. 2.— Color blackbody temperature of burst spectra for 26 bursts from 4U 1728-34 versus flux. Solid curve presents the analytical model fit with fixed $d_{10} = 0.45$ and $Y_{He} = 1.0$. Dashed line present the same model with $Y_{He} = 0$.

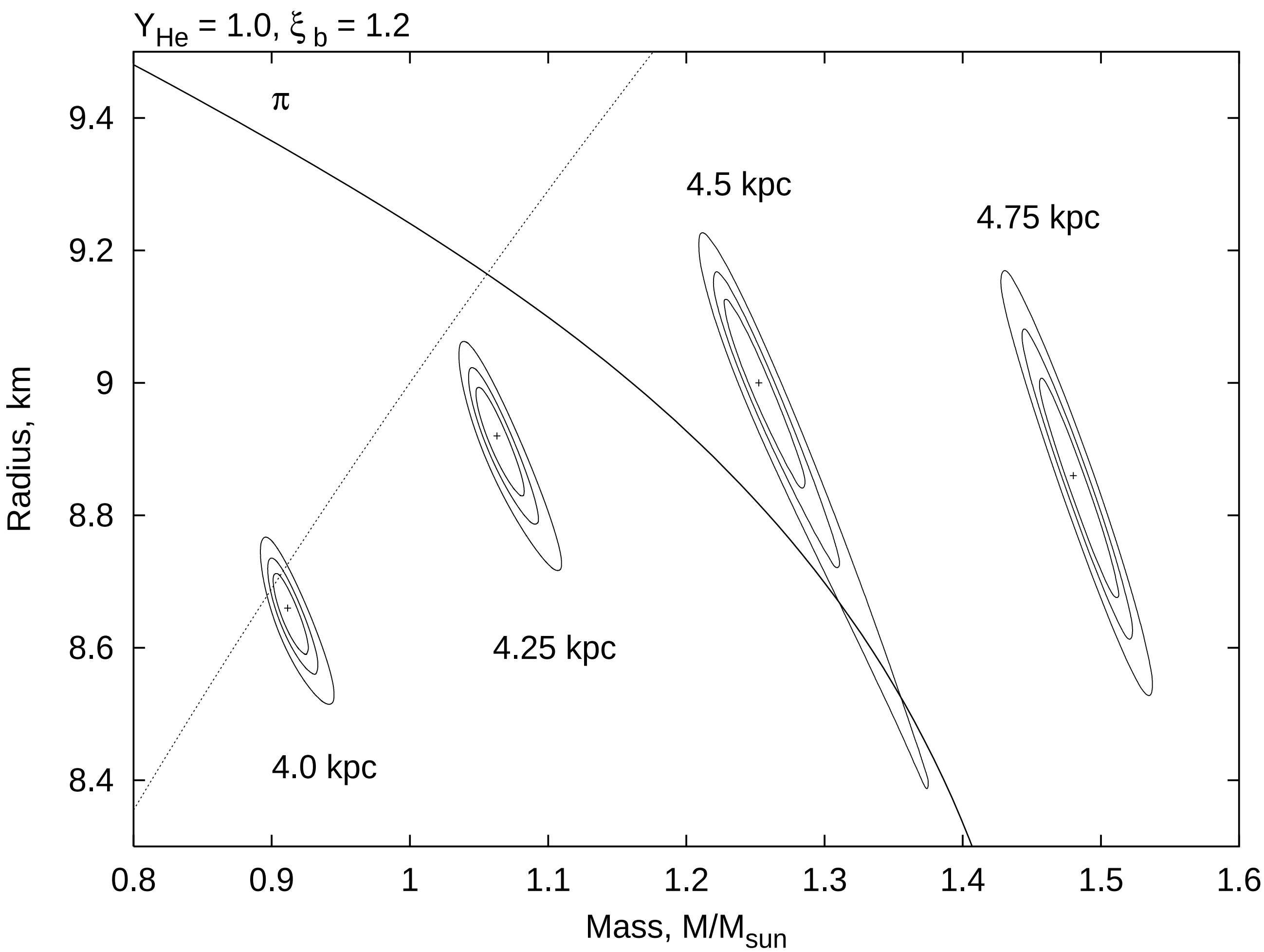

Fig. 3.— Mass-radius contour obtained by the model fitting. Mass-radius relations for soft EOS (Baym & Pethick 1979) is presented by solid line. The dotted curve shows the dependence of the accretion disk inner edge R_{in} obtained using the transition layer model (TLM).